

CALIBRATION OF MECHANISTIC-EMPIRICAL RUTTING MODEL USING IN-SERVICE PAVEMENT DATA FROM THE SPS-1 EXPERIMENT

By

Hassan K. Salama, Ph. D.

Research Associate
Department of Civil and Environmental Engineering
Michigan State University
3546 Engineering Building
East Lansing, Michigan 48824
email: salamaha@egr.msu.edu

Karim Chatti, Ph.D. (Corresponding Author)

Associate Professor
Department of Civil and Environmental Engineering
Michigan State University
3546 Engineering Building
East Lansing, Michigan 48824
phone: 517-355-6534; fax: 517-432-1827
email: chatti@egr.msu.edu

Syed W. Haider, Ph. D.

Research Associate
Department of Civil and Environmental Engineering
Michigan State University
3546 Engineering Building
East Lansing, Michigan 48824
email: syedwaga@egr.msu.edu

Prepared for presentation and publication
at the

2006 Annual Meeting of TRB
Washington, D.C.

November 21, 2005

No. of figures = 6 x 250 = 1500 word equivalents

No. of tables = 5 x 250 = 1250 word equivalents

Text = 5,185 words

Total = 7,935 words

ABSTRACT

This paper presents the results from multivariate regression analyses on rut data from the SPS-1 experiment in the Long Term Pavement Performance (LTPP) program to develop models for predicting permanent deformation parameters (α and μ) for a three-layer pavement system (asphalt concrete, base and subgrade). All available material, structural and climatic data used to explain rutting were extracted from the LTPP database. Using simple linear regression, α and μ were regressed against these independent variables. The variables that have reasonable relationships (relatively higher R^2) were introduced into the multiple linear regression models. The backward regression analysis was used to select the statistically significant variables for the final models.

The variables selected for AC rutting included the strain at the middle of the AC layer, % passing sieve number 10 and % voids filled with asphalt of the most upper AC layer, the average of daily maximum air temperatures for the year, and the freezing index. A total of 15 out of 109 sections were used for predicting α_{AC} and μ_{AC} . This is due to the limited amount of available data to calculate VTM, VFA, and VMA, which are important for explaining the rate of the AC rutting. The variables selected for base rutting included the backcalculated base modulus, thickness of the base layer, % passing sieve number 200, a newly developed weighted average gradation index, and the strain at the middle of the base layer. A total of 27 out of 109 sections were used for predicting α_{base} and μ_{base} . The variables selected for subgrade rutting included the strain at the middle of the first 40 inches of subgrade, a weighted gradation index and the plasticity index of the subgrade, the number of days above 32.2 °C, the number of days with more than 0.25 mm precipitation, and the backcalculated subgrade modulus. A total of 17 out of 109 sections were used for predicting $\alpha_{subgrade}$ and $\mu_{subgrade}$.

In general, the α -prediction models for all layers are more precise than those for μ . This could be due to the fact that the α and μ values were backcalculated from time-series data, which show the rate of growth in rut depth over time. Also it should be noted that μ -values for the AC and base layers were significantly affected (positively) by their corresponding α -values. This implies that pavements with lower μ -values (lower initial rutting) will show lower α -values (higher rut growth with time) and vice-versa.

INTRODUCTION

Since rutting is a major failure mode in flexible pavements, researchers have been trying to predict rut depth for future rehabilitation and budget allocation. There are two main approaches for the prediction of rutting: 1) subgrade strain model (i.e. AI and Shell models) and 2) permanent deformation within each layer. The first approach assumes that most of the rutting results from the subgrade layer only, and is no longer valid based on observations from the field. The second approach considers the rutting contribution from all pavement layers, and is not widely used due to the difficulties in determining the elasto-plastic characteristics of pavement materials. Due to increased tire pressures and new axle configurations as well as observations from the field, researchers began to investigate the rutting contribution from all pavement layers. This approach is also implemented in the new mechanistic-empirical (ME) pavement design guide.

One of the main models related to this approach is the VESYS rutting model (1) that relates the plastic strain to the elastic strain through the permanent deformation parameters (PDPs) μ and α as follows:

$$\varepsilon_p(n) = \mu \varepsilon_e n^{-\alpha} \quad (1)$$

where

- $\varepsilon_p(n)$ = the permanent or plastic strain at the n^{th} load application,
- ε_e = the elastic or resilient strain at 200 repetitions,
- n = the number of load applications,
- α = permanent deformation parameter indicating the rate of decrease in permanent deformation (hardening) as the number of load applications increases ($0 < \alpha \leq 1$),
- μ = permanent deformation parameter representing the constant of proportionality between plastic and elastic strain ($\mu > 0$). Values greater than 1 indicate premature rutting.

The total rut depth can be obtained by integrating Equation 1 over n , multiplying the average vertical elastic strain at the center of each layer by its thickness, and summing the deformations over all layers:

$$\rho_p = h_{AC} \frac{\mu_{AC}}{1-\alpha_{AC}} \left(\sum_{i=1}^K (n_i)^{1-\alpha_{AC}} (\varepsilon_{ei,AC}) \right) + h_{base} \frac{\mu_{base}}{1-\alpha_{base}} \left(\sum_{i=1}^K (n_i)^{1-\alpha_{base}} (\varepsilon_{ei,base}) \right) + h_{SG} \frac{\mu_{SG}}{1-\alpha_{SG}} \left(\sum_{i=1}^K (n_i)^{1-\alpha_{SG}} (\varepsilon_{ei,SG}) \right) \quad (2)$$

- ρ_p = total cumulative rut depth (in the same units as the layer thickness),
- i = subscript denoting axle group,
- K = number of axle group,
- h = layer thickness for AC layer, combined base layer, and subgrade layer, respectively,
- n = number of load applications,
- ε_e = compressive vertical elastic strain at the middle of the layers,
- μ = permanent deformation parameter representing the constant of proportionality between plastic and elastic strain, and
- α = permanent deformation parameter indicating the rate of change in rutting as the number of load applications increases.

The most essential task in using this model is to accurately predict μ and α for each pavement layer within the pavement system. The permanent deformation parameters, PDPs can be predicted using laboratory (2) or field data. Once the PDPs are determined, Equation 2 can be used to decompose the total rutting into percentages for each pavement layer.

Ali *et al.*, 1998 (3) calibrated the new form of the model using 61 sections from the Long Term Pavement Performance (LTPP) General Pavement Study 1 (GPS-1) by backcalculating the permanent deformation parameters for each layer. Ali and Tayabji, 2000 (4) also proposed using a transverse profile to backcalculate permanent deformation parameters, and reported one set of values obtained from only one LTPP section. Kenis, 1997 (5) used Accelerated Pavement Test (APT) performance data to validate and calibrate the two flexible pavement rutting models used in VESYS 5. In their study, they suggested a range for the permanent deformation parameters for the pavement layers. Eventhough several attempts have been made to estimate these parameters, agreement between studies varies.

Simpson *et al.*, 1994 (6) developed a rutting model to predict the total rut depth for LTPP data (GPS-1 and GPS-2). The model uses a multiplicative regression equation and includes several variables including environmental conditions, material properties, pavement layer cross section, and construction quality. In a further study, Simpson *et al.*, 1995 (7) distinguished the rutting contribution from each pavement layer using the same LTPP data. A general model for the total surface rutting, subgrade rutting, base rutting, AC rutting, and heave was generated using neural network analysis. The variables that were considered in each model are listed in Table 1.

RESEARCH OBJECTIVES

The main objective of this paper is to develop regression models for predicting permanent deformation parameters α and μ for the VESYS empirical-mechanistic rut model. The variables included in the model are pavement layer material properties, climatic-based indices and pavement structural parameters. All the data used in this analysis are from the Long Term Pavement Performance (LTPP) SPS-1 experiment. A total of 109 pavement sections with time series rut data totaling 724 data points were considered in the analysis. The calibrated variables α and μ were obtained using a Backcalculation scheme that involved iterating over trial values using commercially available “Solver” in Excel Microsoft software. The details of the Backcalculation analysis are described elsewhere (8, 9). A brief summary of the analysis follows.

BACKCALCULATION OF PDPs

Salama *et al.*, 2005 (8) backcalculated the PDPs by matching the rut time series data from the SPS-1 experiment in the LTPP program. The most novel aspect of this backcalculation process involved the application of the approach developed in NCHRP 468 (10), which uses transverse surface profiles to locate the layer causing most of rutting. Using this process, the most likely solution for these parameters was attained for 109 pavement sections within the SPS-1 experiment. Figure 1 shows predicted versus measured rut depth. The backcalculated PDPs needed for matching the time series rut data were considered as the “actual” values since the match was very good ($R^2 = 0.929$, $SE = 0.04\text{mm}$).

AVAILABLE MATERIAL PROPERTIES

The LTPP database provides information for the pavement layers of all SPS-1 experiment sections, structural, material as well as climatic variables. Several data elements were extracted for each pavement layer from release 17 of the LTPP database (datapave.com) as follows:

- AC layer
 - The gradation of the fine and coarse aggregate,
 - Bulk specific gravity of fine and coarse aggregate,
 - Bulk specific gravity of the asphalt mixture from field cores,
 - Maximum theoretical specific gravity of the HMA mixture,
 - AC binder content,
 - Kinematic and absolute viscosity of the asphalt binder
 - Indirect tensile strength of the HMA mixture,
 - Resilient modulus of the HMA mixture.
- Base layer
 - The gradation of the fine and coarse aggregate,
 - Atterberg limits (liquid and plastic limits).
- Subgrade layer
 - Gradation,
 - Moisture content,
 - Atterberg limits (liquid and plastic limits),
 - Unconfined compressive strength of the clay.

Using the AC layer data, the voids in total mix (VTM), voids in mineral aggregate (VMA), and voids filled with asphalt (VFA) were calculated using the HMA volumetric equations (9 and 11). Several climatic variables were extracted from the SPS-1 data and considered in the regression analysis as follows:

- Mean annual temperature,
- Maximum annual temperature,
- Minimum annual temperature,
- Days above 32 °C,
- Days below 0 °C,

- Freeze index,
- Freeze thaw cycle,
- Total annual precipitation,
- Wet days,
- Intense precipitation days/year.

More detail descriptions of the climatic variables can be found elsewhere (12). The pavement layer thicknesses from the backcalculation procedure and the strain at the middle of each pavement layer (calculated using the KENLAYER program (13)) were considered as independent variables in the regression analysis. Since the independent variables are many, not all are introduced in the multiple linear regression analysis. Based on previous studies (8 and 9) along with the simple univariate linear regression of each variable, the independent variables that have reasonable relationships with the PDPs were selected and introduced in the model. Additionally, the backward regression analysis was used to select the most statistically significant variables for each permanent deformation parameter.

REGRESSION ANALYSIS

In this paper, the multiplicative form of multiple linear regression was utilized to oversee the nonlinear relationship between the PDPs and the independent variables. Using this multiplicative model requires the dependent variable to be regressed on the natural logarithm of the independent variables; for more detail see (6). Several precautions were taken into consideration to ensure integrity of the model as follows:

- The signs of the multiple linear regression coefficients should agree with the signs of the simple linear regression of the individual independent variables,
- The signs of the multiple linear regressions for each independent variable should agree with intuitive engineering judgment. For example, higher annual temperature should increase the rate of the rutting in AC layer, and therefore create more positive values for $(1-\alpha)$ and μ .
- There should be no multicollinearity among the final selected independent variables. For example, two independent variables having the same effect (high bivariate correlation) on the dependent variable should not be included in one model at the same time.
- One of several variable selection algorithms (e.g. stepwise, forward, and backward regression analyses) was used in regression to eliminate the statistically insignificant independent variables for each of the six models. For example, for the AC layer, the α model started with average of daily maximum air temperatures, percent passing sieve number 10, percent voids filled with asphalt, vertical compressive strain at the middle of AC layer, kinematic viscosity of the asphalt binder at 275 F, percent asphalt content, and asphalt concrete layer thickness and ended up with only vertical compressive strain at the middle of AC layer, percent passing sieve number 10, percent voids filled with asphalt, and average of daily maximum air temperatures remaining as significant contributors to the model after a backward regression analysis (see equation 3). For more detail on the variable selection, see (6).
- The model with the smallest number of independent variables, minimum standard error, and highest R^2 value was selected.

In addition, after finalizing the model for each permanent deformation parameter, the regression models were tested to ensure there were no assumption violations. These tests are:

- Normality distribution,
- Constant variance,
- Cook's distance.

Asphalt Concrete Layer Regression Analysis

The rutting in the AC layer is characterized by α_{AC} and μ_{AC} . The parameter, α_{AC} , represents the rate of decrease in AC rutting as the number of load applications increases and as the material becomes stiffer (the hardening effect due to environmental conditions). The parameter, μ_{AC} , represents the constant of proportionality between plastic and elastic strain within the AC layer.

There are several factors affecting AC rutting. All available material and climatic data used to explain AC rutting (8 and 9) were extracted from the LTPP database. Using simple linear regression, α_{AC} and μ_{AC} were regressed against these independent variables. The variables that have reasonable relationships (relatively higher R^2) were introduced into the multiple linear regression models. The backward regression analysis was used to select the statistically significant variables for the final model. A total of 15 out of 109 sections were used for predicting α_{AC} and μ_{AC} . This is due to the limited amount of available data to calculate VTM, VFA, and VMA, which are important for explaining the rate of the AC rutting. Equations 3 and 4 show the final model for α_{AC} and μ_{AC} .

$$\alpha_{AC} = 5105.124 * (\text{Strain})^{0.555} * P_{10}^{-1.013} * (VFA)^{-0.58} * (MAAT)^{0.732} \quad (3)$$

$$\mu_{AC} = 6.746 * \alpha_{AC}^{4.102} * FI^{-0.213} \quad (4)$$

where:

<i>Strain</i>	= strain at the middle of AC layer due to ESAL
<i>P</i> ₁₀	= % passing sieve number 10 of the most upper AC layer
<i>VFA</i>	= % voids filled with asphalt of the most upper AC layer
<i>MAA T</i>	= Average of daily maximum air temperatures for year, °C
<i>FI</i>	= freezing index

It can be seen from the equations that α_{AC} is a function of P_{10} and VFA (both material-related properties), *strain* (structure-related), and $MAAT$ (environment-related), while μ_{AC} is a function of α_{AC} (rate of rutting) and FI (environment-related). This implies that, in order to predict μ_{AC} , an estimate for α_{AC} must be predicted first. Attempts were made to predict μ_{AC} from variables other than α_{AC} , but all alternatives to using α_{AC} were found to have much lower R^2 values. Table 2 shows the analysis of variance of the multiple linear regressions of α_{AC} and μ_{AC} . The table shows the degrees of freedom (the number of sections used, minus one), the sum of squares and mean square errors, the F-test results, and the p -value (significance) for each model. The results show that the overall models for α_{AC} and μ_{AC} (as well as for base and subgrade layers) are statistically significant. Table 3 shows 90% and 79% variance for the natural logarithm-based, multiplicative models of α_{AC} and μ_{AC} , respectively.

Table 4 shows the unstandardized and standardized model coefficients, t -test, statistical significance, and collinearity statistics for both α_{AC} and μ_{AC} . It can be seen from the table that all independent variables included in the model for both α_{AC} and μ_{AC} are statistically significant. Also, there was no concern about the multicollinearity (small variance inflation factor, VIF). Moreover, there is a good agreement between the multiple linear regression coefficient signs and the univariate relationships of the individual variables. The standardized regression coefficients show that:

- The higher the initial strain or the $MAAT$, the higher the α_{AC} value, which means a lower rate of rutting progression with time (the exponent is $1-\alpha_{AC}$). In other words, if the AC layer is soft (higher initial strain) or the climatic region is hot (higher temperatures), the majority of the rutting will occur at the initial stage and taper off with the remaining life of the pavement.
- The higher the percent passing sieve number 10 or the percent of voids filled with asphalt, the lower the α_{AC} value, which means a higher rate of rutting progression with time. In other words, rutting will be more pronounced if the AC layer is composed of a finer mix or it contains more voids.
- The higher the α_{AC} , the higher the μ_{AC} . This means that pavements with lower initial rutting (lower μ_{AC} value) will show rutting over a longer period of time (lower α_{AC} value).
- The higher the freezing index for a region, the lower its μ_{AC} values. This indicates that unlike hotter regions, pavements constructed in colder regions will show lower initial rutting.

The standardized regression coefficients were used to rank the importance of the independent variables to α_{AC} and μ_{AC} values, as shown in Table 4.

Figure 2 shows the actual versus predicted α_{AC} and μ_{AC} . The “actual” values are previously determined through backcalculation using SPS-1 time-series data (6 and 10). It can be seen from the figure that the prediction of α_{AC} is significantly higher than that of μ_{AC} . Note, however, that reasonable prediction of μ_{AC} were possible at lower values ($\mu < 0.5$). Also, note that good prediction of μ_{AC} at higher values (>1) is not expected since higher μ_{AC} values represent higher initial AC rutting due to specific problems (material-or construction-related). R^2 - values shown in Figure 2 correspond to original scale, and are lower than the model R^2 -values shown in Table 3.

Table 5 shows the descriptive statistics for α_{AC} , μ_{AC} and their independent variables used in the regression analyses. It should be noted that Equations 3 and 4 should be used within the range for each variable listed in Table 5 in order to obtain reasonable predictions.

Base Layer Regression Analysis

For the base layer, the only data available were the gradation, base thickness used in the backcalculation, and the calculated strain at the middle of the base due to one standard axle. Unlike the AC layer, in which the materials are highly controlled, the base and subgrade layers of flexible pavements are frequently more dissimilar from one section to another. This becomes evident when examining sieve analyses. Figure 3 shows how the AC layer-content is much more consistent than that of the base and subgrade layers, since consistency of layer material across sites (each curve represents one site) can be ascertained by the uniformity of the graphs. Since the content of AC material is highly controlled, a particular sample can be uniquely identified by an individual sieve measurement, that is, the percent material passing through one particular sieve (see Figure 3 (a)). This is not the case for the base layer material, since base materials from two different sections might have the same percent passing through one sieve and different gradations for the other sieves, as shown in Figure 3 (b). Therefore, while a single sieve percentage (amount passing sieve #10) was selected by the AC layer regression as significant, a new index, termed Gradation Index (GI), is introduced in this analysis to represent the gradation of the base layer such that using the GI alone or with the percent passing of any given sieve (such as sieve 4, 10, or 200) will be more representative of an individual base layer's material. The GI can be calculated from the following equation:

$$GI = \frac{\sum p * \log SS}{\sum \log SS} \quad (5)$$

where

p = % passing of the individual sieve, and
 $\log SS$ = logarithm of sieve size in mm.

For the base regression analysis, only sections that have base rutting of 10 percent or more out of the total surface rutting and available base gradations were considered; these total 27 out of 109 sections. The final regression equations for predicting the α_{base} and μ_{base} are shown below:

$$\alpha_{base} = 2.724 * 10^{-5} * \text{modulus}^{0.102} * \text{Thickness}^{0.066} * P_{200}^{-0.098} * GI^{1.982} \quad (6)$$

$$\mu_{base} = 7.1977 * 10^{-3} * \alpha_{base}^{6.256} * \text{Thickness}^{-0.808} * \text{strain}^{-0.809} \quad (7)$$

where

Modulus = backcalculated base modulus, psi
 Thickness = Thickness of base layer used in the backcalculation, in
 P_{200} = % passing sieve number 200
 GI = Gradation index
 Strain = Strain at the middle of the base layer due to one standard axle

Table 2 shows the analysis of variance of the multiple linear regression for α_{base} and μ_{base} . The results show that the overall models for α_{base} and μ_{base} are statistically significant. Table 3 shows that 50.6 % and 68.7 % of the variance for $\ln(\alpha_{base})$ and $\ln(\mu_{base})$, respectively, is explained by \ln of the independent variables.

Table 4 shows the unstandardized and standardized model coefficients, t -test, statistical significance, and collinearity statistics for both α_{base} and μ_{base} . It can be seen from the table that all independent variables included in the model for both α_{base} and μ_{base} are statistically significant except for the base thickness in the α_{base} model. Excluding the base thickness from the model causes a dramatic reduction of R^2 ; therefore base thickness was kept in the model. Also, there was no concern about multicollinearity (small VIF). Moreover, there is a good agreement between the multiple linear regression coefficient signs and the univariate relationships of the individual variables. The standardized regression coefficients show that:

- The higher the initial modulus, the higher the α_{base} value, which means a lower rate of rutting progression with time (the exponent is $1-\alpha_{base}$).
- The thicker the base or higher GI (coarser material), the higher the α_{base} , which means a lower rate of base rutting with time.
- The higher the percent passing sieve 200, the lower the α_{base} , which leads to a higher rate of rutting with time.

- Similar to the AC layer, there is a strong relationship between α_{base} and μ_{base} ($R^2 = 0.5949$); the higher the α_{base} the higher the μ_{base} . This means that a pavement with lower initial rutting (lower μ_{base} value) will show rutting over a longer period of time (lower α_{base} value).
- The thicker the base layer or higher initial strain value, the lower the μ_{base} , which indicates that rutting will keep progressing with time.

The standardized regression coefficients were used to rank the importance of the independent variables in the α_{base} and μ_{base} models, as shown in table 4. Figure 4 shows the actual versus predicted α_{base} and μ_{base} . It can be seen that similarly to the AC layer, there is better prediction for α_{base} than for μ_{base} . Also, the prediction of μ_{base} worsens at higher μ_{base} values. Again, note that, higher μ_{base} -values ($\mu_{\text{base}} > 1$) are indicative of premature rutting which could be caused by specific material-or construction-related problem. Table 5 shows the descriptive statistics of α_{base} , μ_{base} and their independent variables used in the regression analysis. It should be noted that Equations 6 and 7 should be used within the range of the data in Table 5 to obtain reasonable predictions.

Subgrade Regression Analysis

Similar to the base layer and even more pronounced, the percent subgrade material passing through one sieve is not enough to characterize the subgrade materials, as shown in Figure 3 (c). Therefore, the need for the GI (Equation 5) is at least as great for the subgrade regression analysis as it was for the base layer.

For subgrade analysis, only those sections that show rutting in the subgrade and have α_{SG} values less than 0.9 were considered, totaling 17 out of 109 sections. The final regression equations for predicting α_{SG} and μ_{SG} are shown below:

$$\alpha_{\text{SG}} = 1.385 \times 10^{-5} * \text{strain}^{0.043} * \text{GI}^{1.89} * \text{PI}^{0.116} * \text{D}_{32}^{0.14} * \text{FI}^{0.036} * \text{wet days}^{0.326} \quad (8)$$

$$\mu_{\text{SG}} = 2.575 * 10^{-63} * \text{modulus}^{2.41} * \text{strain}^{-0.764} * \text{GI}^{22.594} * \text{PI}^{1.304} \quad (9)$$

where

Strain	= Strain at the middle of the first 40 inches of subgrade layer due to one ESAL
GI	= Gradation index (as calculated from equation 5)
PI	= Plasticity index of subgrade layer
D_{32}	= Number of days where daily maximum air temperature is above 32.2 °C for year
Wet days	= Number of days for which precipitation was greater than 0.25 mm for year.
Modulus	= backcalculated subgrade modulus, psi

Table 2 shows the analysis of variance for α_{SG} and μ_{SG} . The results show that the overall models for α_{SG} and μ_{SG} are statistically significant. Table 3 shows that 47.3% and 84.8% of the variance for $\ln(\alpha_{\text{SG}})$ and $\ln(\mu_{\text{SG}})$, respectively, is explained by \ln of the independent variables. Table 4 shows the unstandardized and standardized model coefficients, t -test, statistical significance, and collinearity statistics for both α_{SG} and μ_{SG} . It can be seen from the table that all independent variables included in the model for both α_{SG} and μ_{SG} are statistically significant except for the strain and FI in the α_{SG} model. Excluding either of these variables from the model causes a dramatic reduction of the R^2 value; therefore, similar to the base layer, they were kept in the model since the backward regression analysis selects them. Also, there was no concern about multicollinearity (small VIF). Moreover, there is a good agreement between the multiple linear regression coefficient signs and the univariate relationship of the individual variables. The standardized regression coefficients (Table 4) show that:

- The higher the PI, GI, D_{32} , wet days, FI, and vertical compressive strain at the middle of the first 40 inches (1016 mm) of the subgrade, the higher the α_{SG} , which means a lower rate of rutting progression with time (the exponent is $1 - \alpha_{\text{SG}}$).
- The higher the PI, GI, and subgrade modulus, the higher the μ_{SG} , which means a majority of the resulting rutting will occur at the first stage of pavement life with very little progression with time. Similar to the base layer, higher initial strain value in the subgrade indicates that rutting will keep progressing with time. Figure 5 shows the actual versus prediction of α_{SG} and μ_{SG} . The prediction of α_{SG} and μ_{SG} are reasonable, although the later prediction worsens at higher μ_{SG} -values. As mentioned above, these are indicative of early rutting, which could be due to material-or construction-related problems.

Table 5 shows the descriptive statistics of α_{SG} , μ_{SG} and the independent variables used in the regression analysis. Similar to the AC and base layers, Equations 8 and 9 should be used within the range of the data in Table 5 to obtain reasonable predictions.

To verify the total surface rutting prediction, Figure 6 shows the field versus predicted total surface rut depth for section SPS-1 50113. The predicted rut depth was calculated using Equation 2 and the PDPs for all pavement layers were calculated through equations 3, 4, 6, 7, 8 and 9.

Finally, it is interesting to note that, using Equation 2 to decompose the total rutting, a majority of the total rutting occurs within the AC layer (on average, 57%), followed by the base layer (27.5%) and the subgrade layer (15.5%) for SPS-1 experimental sections. This is paralleled by the fact that the base and subgrade layers have successively more variables available within the predictive models than the AC layer. Also, the AC regression analysis showed that the overall model for α_{AC} and μ_{AC} are statistically significant, as are all variables included. On the other hand, the overall models for α_{base} and μ_{base} are statistically significant, with only one insignificant variable (base thickness). Following the same pattern of decreased significance with decreased rutting percentage, the overall models for α_{SG} and μ_{SG} are statistically significant, yet contain two insignificant variables (strain and FI). This understandable pattern suggests the need for more study and further theorizing of variables to explain rutting within the base and subgrade layers.

CONCLUSION

Three sets of regression equations relating the permanent deformation parameters α and μ of the AC, base and subgrade layers, respectively, were developed using multivariate regression analyses on rut data from the SPS-1 experiment in the Long Term Pavement Performance (LTPP) program. All available material, structural and climatic data used to explain rutting were extracted from the LTPP database. Using simple linear regression, α and μ were regressed against these independent variables. The variables that have reasonable relationships (relatively higher R^2) were introduced into the multiple linear regression models. The backward regression analysis was used to select the statistically significant variables for the final models.

The variables selected for AC rutting included the strain at the middle of the AC layer, % passing sieve number 10 and % voids filled with asphalt of the most upper AC layer, the average of daily maximum air temperatures for the year, and the freezing index. A total of 15 out of 109 sections were used for predicting α_{AC} and μ_{AC} . This is due to the limited amount of available data to calculate VTM, VFA, and VMA, which are important for explaining the rate of the AC rutting. The variables selected for base rutting included the backcalculated base modulus, thickness of the base layer, % passing sieve number 200, a newly developed weighted average gradation index, and the strain at the middle of the base layer. A total of 27 out of 109 sections were used for predicting α_{base} and μ_{base} . The variables selected for subgrade rutting included the strain at the middle of the first 40 inches of subgrade, a weighted gradation index and the plasticity index of the subgrade, the number of days above 32.2 °C, the number of days with more than 0.25 mm precipitation, and the backcalculated subgrade modulus. A total of 17 out of 109 sections were used for predicting $\alpha_{subgrade}$ and $\mu_{subgrade}$.

In general, the α -prediction models for all layers are more precise than those for μ . This could be due to the fact that the α and μ values were backcalculated from time-series data, which show the rate of growth in rut depth over time. Also it should be noted that μ -values for the AC and base layers were significantly affected (positively) by their corresponding α -values. This implies that pavements with lower μ -values (lower initial rutting) will show lower α -values (higher rut growth with time) and vice-versa.

REFERENCES

1. Moavenzadeh, F., J. E. Soussou, H. K. Findakly, and B. Brademeyer. (1974). "Synthesis for rational design of flexible pavement." FH 11-776, Federal Highway Administration.
2. Qi, X. and M. W. Witczak, "Time-Dependent Permanent Deformation Models for Asphaltic Mixtures," Transportation Research Board 1639, 1998, PP 83-93.
3. Ali, H. A., S. D. Tayabji, and F. L. Torre, "Calibration of mechanistic-empirical rutting model for in-service pavements," *Transportation Research Record (1629)*, pp. 159-168, 1998.
4. Ali, H. A. and S. D. Tayabji, "Using transverse profile data to compute plastic deformation parameters for asphalt concrete pavements," *Transportation Research Record*, pp. 89-97, 2000.

5. Kenis, W. and W. Wang, "Calibrating Mechanistic Flexible Pavement Rutting Model from Full Scale Accelerating Tests," presented at *8th International conference on asphalt pavement*, Seattle, Washington, 1997, pp. 663-672.
6. Simpson A. L., J. B. Rauhut, P. R. Jordahl, E. Owusu-Antwi, M. I. Darter, R. Abroad, O. J. Pendleton, and Y. Lee, (1994) "Sensitivity Analyses for Selected Pavement Distresses" SHRP report No. SHRP-P-393.
7. Simpson, A. L., J. F. Daleiden, and W. O. Hadley (1995) "Rutting analysis from a different perspective" Transportation research record 1473, pp 9-16.
8. Salama, H. and K. Chatti, and S. Haider "Backcalculation of Permanent Deformation Parameters Using Time series Rut Data from In-service Pavement in the LTPP SPS-1 Experiment" accepted for presentation and recommended for publication for Transportation Research Board meeting, January 2006.
9. Salama, H. and "Effect of heavy multiple axle trucks on flexible pavement rutting," Ph. D. Dissertation, Civil and Environmental Engineering, Michigan State University, East Lansing, Michigan, 2005.
10. White, T. D., E. H. John, J. T. H. Adam, and F. Hongbing, "Contribution of Pavement Structural Layers to Rutting of Hot Mix Asphalt Pavements," NCHRP, Washington, DC. Report 468, 2002.
11. Roberts, F. L., P. S. Kandhal, E. R. Brown, D. Y. Lee, and T. W. Kennedy, "Hot Mix Asphalt Materials, Mixture, Design, and Construction," Second Edition, 1996, NAPA Education Foundation, Lanham, Maryland.
12. <http://www.datapave.com/>
13. Huang, Y. H., Pavement Analysis and Design, 2nd Edition ed. Upper Saddle River, NJ 07458: Pearson Prentice Hall, 2004.

LIST OF TABLES

Table 1 Independent variables included in different models (9).....	10
Table 2 ANOVA for permanent deformation parameters of AC, base, and subgrade layers	11
Table 3 Model Summary for permanent deformation parameters of AC, base, and subgrade layers.....	11
Table 4 Model coefficients for permanent deformation parameters of AC, base, and subgrade layers.....	12
Table 5 Descriptive statistics of PDPs and their variables.....	13

LIST OF TABLES

Figure 1 Field versus predicted total surface rut depth.....	14
Figure 2 Actual versus predicted PDPs for AC layer	15
Figure 3 Sieve analysis: (a) AC layer, (b) base layer, and (c) Subgrade layer.....	16
Figure 4 Actual versus predicted PDPs for base layer.....	17
Figure 5 Actual versus predicted PDPs for subgrade layer	18
Figure 6 Field versus predicted total surface rut depth for section SPS-1 50113	19

Table 1 Independent variables included in different models (9)

Total surface rutting	Subgrade rutting	Base rutting	AC rutting	Heave
AC thickness Air voids percentage Asphalt viscosity @140°F Annual precipitation Number of days above 90°F Freeze thaw cycles Plasticity Index Subgrade moisture % passing # 200 in subgrade Base thickness ESALs	Annual precipitation Number of days above 90°F Freeze thaw cycles Plasticity Index Subgrade moisture % passing # 200 in subgrade ESALs	Annual precipitation Number of days above 90°F Base thickness Base compaction ESALs	AC thickness Asphalt content Air voids percentage % passing # 4 in AC Asphalt viscosity @140°F Number of days above 90°F ESALs	Annual precipitation Freeze thaw cycles Plasticity Index Subgrade moisture % passing # 200 in subgrade ESALs

Table 2 ANOVA for permanent deformation parameters of AC, base, and subgrade layers

Variable		Sum of Squares	df	Mean Square	F	Sig.
α_{AC}	Regression	1.675	4	0.419	33.604	0.000
	Residual	0.125	10	0.012		
	Total	1.800	14			
μ_{AC}	Regression	16.675	2	8.338	26.065	0.000
	Residual	3.519	11	0.320		
	Total	20.194	13			
α_{Base}	Regression	0.674	4	0.169	7.653	0.001
	Residual	0.485	22	0.022		
	Total	1.159	26			
μ_{Base}	Regression	59.631	3	19.877	20.000	0.000
	Residual	22.859	23	0.994		
	Total	82.490	26			
α_{SG}	Regression	0.152	6	0.025	3.389	0.043
	Residual	0.075	10	0.007		
	Total	0.227	16			
μ_{SG}	Regression	33.212	4	8.303	23.344	0.000
	Residual	4.268	12	0.356		
	Total	37.480	16			

Table 3 Model Summary for permanent deformation parameters of AC, base, and subgrade layers

Variable	R	R ^{2*}	Adjusted R ²	Std. Error of the Estimate
α_{AC}	0.965	0.931	0.903	0.112
μ_{AC}	0.909	0.826	0.794	0.566
α_{Base}	0.763	0.582	0.506	0.148
μ_{Base}	0.850	0.723	0.687	0.997
α_{SG}	0.819	0.670	0.473	0.087
μ_{SG}	0.941	0.886	0.848	0.596

* Note: R² values correspond to the natural logarithm of the multiplicative model form

Table 4 Model coefficients for permanent deformation parameters of AC, base, and subgrade layers

Variables		Unstandardized Coefficients		Standardized Coefficients	t	Sig.	Collinearity Statistics	
		Beta	Std. Error	Beta (rank)			Tolerance	VIF*
α_{AC}	Constant	8.538	1.220		6.997	0.000		
	Strain	0.555	0.071	0.727 (1)	7.820	0.000	0.802	1.247
	% passing # 10	-1.013	0.156	-0.611 (4)	-6.485	0.000	0.781	1.281
	VFA	-0.580	0.238	-0.213 (3)	-2.439	0.035	0.907	1.103
	MAAT	0.732	0.105	0.589 (2)	6.951	0.000	0.966	1.036
μ_{AC}	Constant	1.909	0.419		4.550	0.001		
	α_{AC}	4.102	0.658	0.786 (1)	6.229	0.000	0.995	1.005
	FI	-0.213	0.066	-0.406 (2)	-3.219	0.008	0.995	1.005
α_{Base}	Constant	-10.511	3.519		-2.987	0.007		
	Modulus	0.102	0.037	0.447 (1)	2.751	0.012	0.721	1.387
	Thickness	0.066	0.051	0.205 (3)	1.303	0.206	0.771	1.297
	P200	-0.098	0.032	-0.462 (4)	-3.094	0.005	0.854	1.172
	GI	1.982	0.715	0.429 (2)	2.774	0.011	0.794	1.259
	Constant	-4.934	2.083		-2.369	0.027		
μ_{Base}	α	6.256	0.942	0.742 (1)	6.639	0.000	0.966	1.035
	Thickness	-0.808	0.355	-0.298 (2)	-2.280	0.032	0.707	1.415
	Strain	-0.809	0.254	-0.417 (3)	-3.182	0.004	0.700	1.428
α_{SG}	Constant	-11.187	3.965		-2.822	0.018		
	Strain	0.043	0.031	0.283 (6)	1.391	0.194	0.798	1.252
	GI	1.890	0.805	0.955 (2)	2.348	0.041	0.199	5.020
	PI	0.116	0.035	1.271 (1)	3.342	0.007	0.228	4.387
	D ₃₂	0.140	0.061	0.914 (3)	2.269	0.047	0.203	4.924
	FI	0.036	0.020	0.656 (5)	1.796	0.103	0.247	4.047
	Wet days	0.326	0.105	0.853 (4)	3.109	0.011	0.438	2.281
μ_{SG}	Constant	-144.12	21.825		-6.603	0.000		
	SG modulus	2.410	0.956	0.403 (3)	2.521	0.027	0.371	2.692
	Strain	-0.764	0.274	-0.388 (4)	-2.786	0.016	0.490	2.043
	GI	22.594	5.006	0.890 (2)	4.513	0.001	0.244	4.096
	PI	1.304	0.211	1.118 (1)	6.191	0.000	0.291	3.436

* Variance Inflation Factor

Table 5 Descriptive statistics of PDPs and their variables

Layer	Variable	Mean	Standard Error	Minimum	Maximum
AC	α_{AC}	0.589	0.173	0.207	0.844
	μ_{AC}	0.649	0.675	0.010	2.059
	Strain	6.35E-05	2.73E-05	2.69E-05	1.03E-04
	P ₁₀	37	8	24	49
	VFA	51.6	6.8	38.5	67.3
	Max AT	22	6	12	29
	FI	158	273	1	988
Base	μ_{base}	0.60	0.77	0.01	2.44
	α_{base}	0.76	0.16	0.50	0.99
	modulus	45058	41131	4599	178098
	thickness	21.7	11.0	3.6	43.3
	Strain	1.38E-04	1.21E-04	1.29E-05	5.07E-04
	P ₂₀₀	29.1	31.5	5.9	91.3
	GI	106.59	4.86	98.38	115.99
SG	μ_{SG}	0.22	0.41	0.01	1.67
	α_{SG}	0.74	0.08	0.56	0.85
	modulus	31189	7827	16846	48495
	strain	4.578E-05	3.171E-05	1.014E-05	1.077E-04
	GI	109.94	6.62	100.86	120.13
	PI	13.82	12.21	1.00	39.00
	D32	61.12	35.66	8.43	153.43
	FI	168.31	202.53	0.74	667.27
	Wet days	112.87	34.34	75.04	163.43

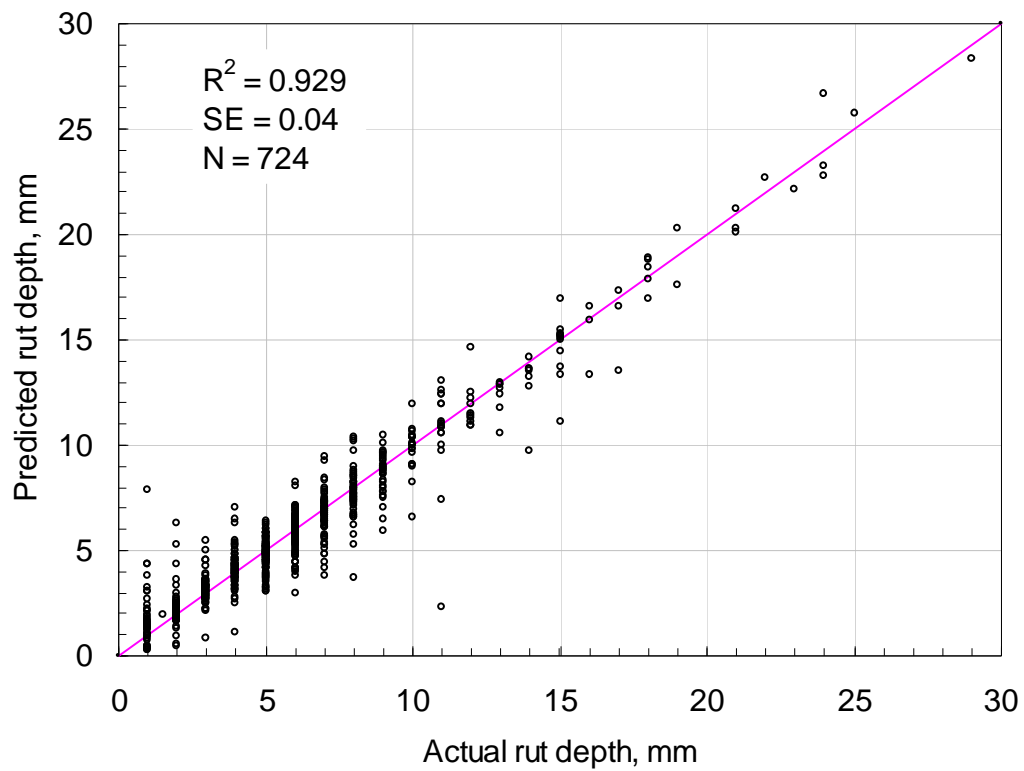
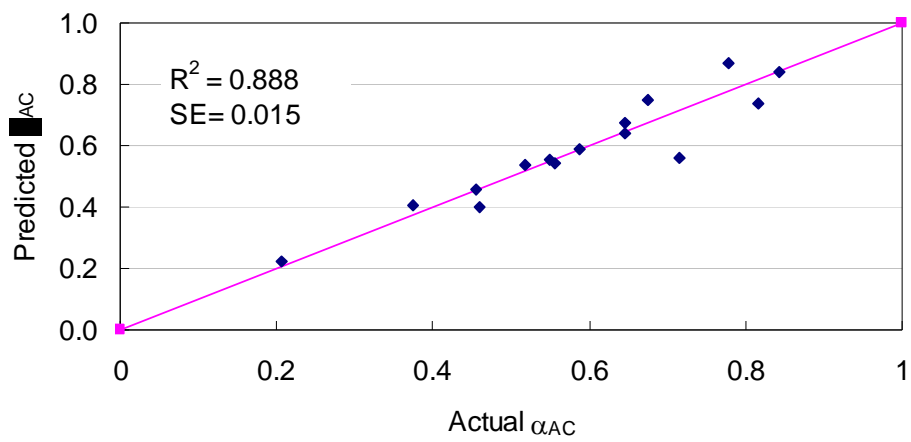
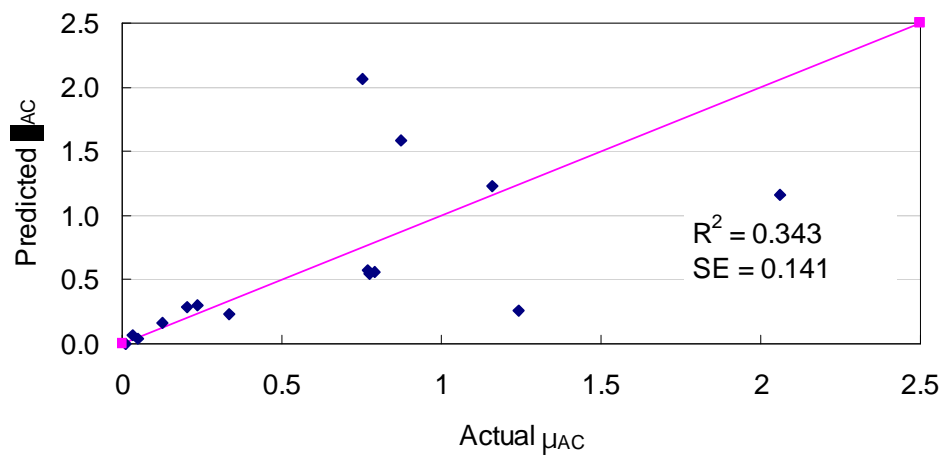


Figure 1 Field versus predicted total surface rut depth

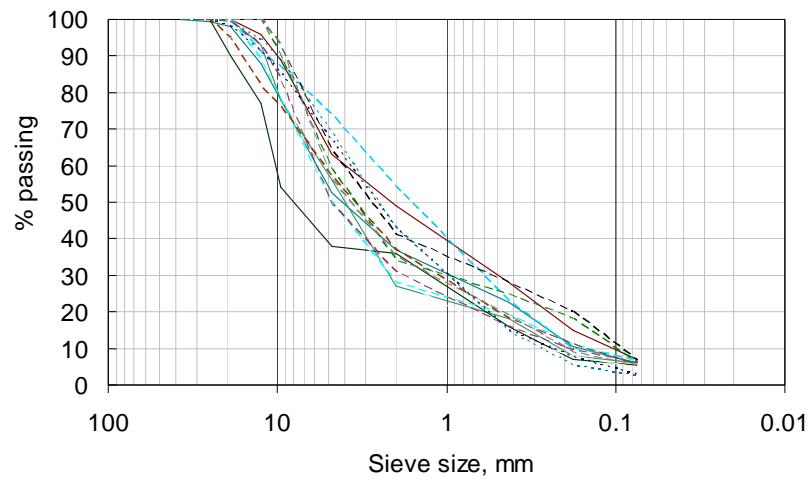


(a) α_{AC}

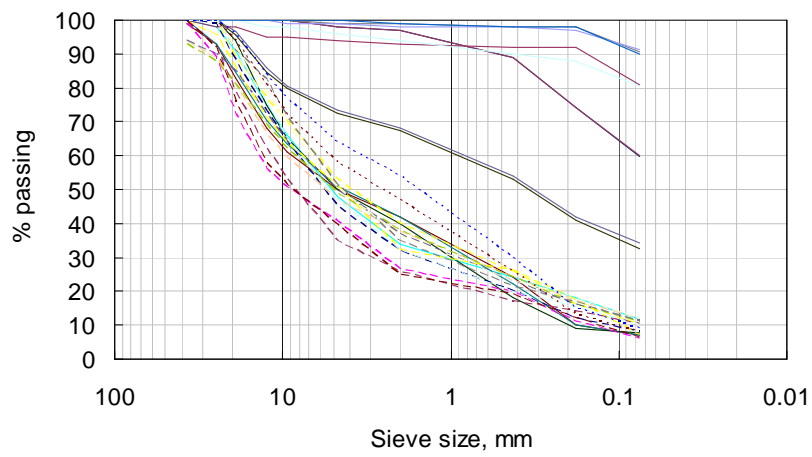


(b) μ_{AC}

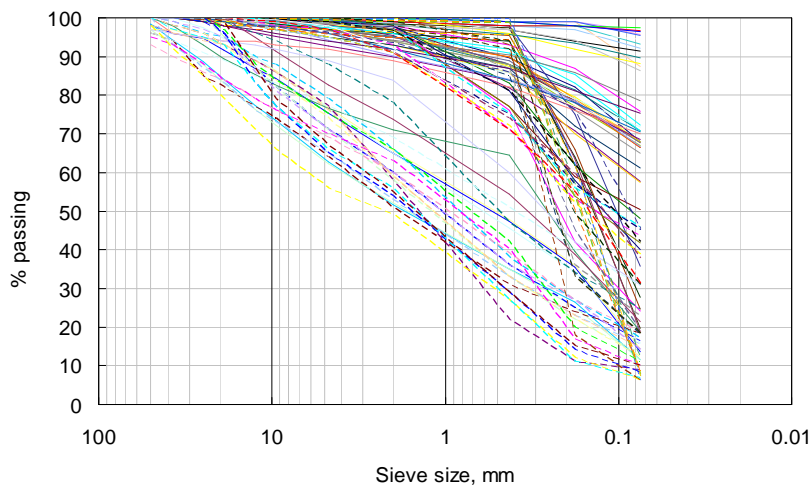
Figure 2 Actual versus predicted PDPs for AC layer



(a)

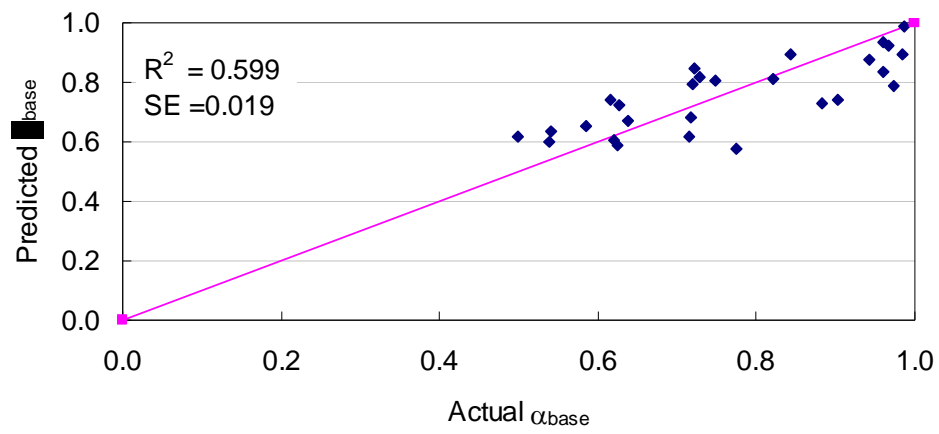


(b)

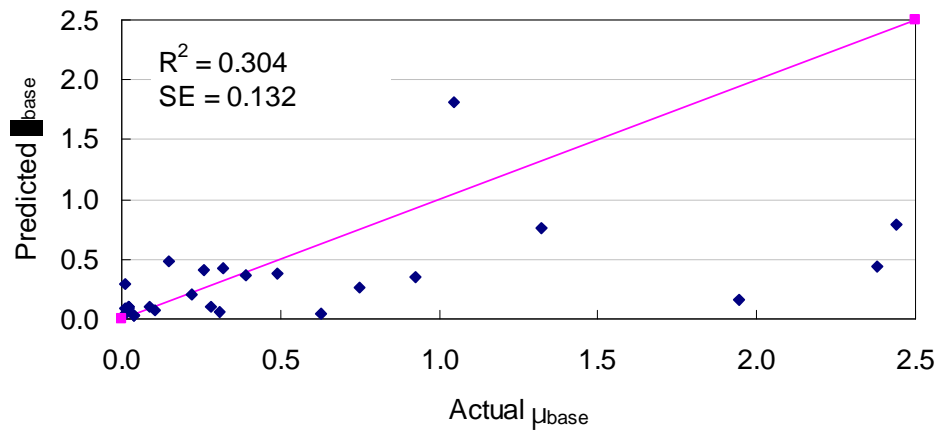


(c)

Figure 3 Sieve analysis: (a) AC layer, (b) base layer, and (c) Subgrade layer

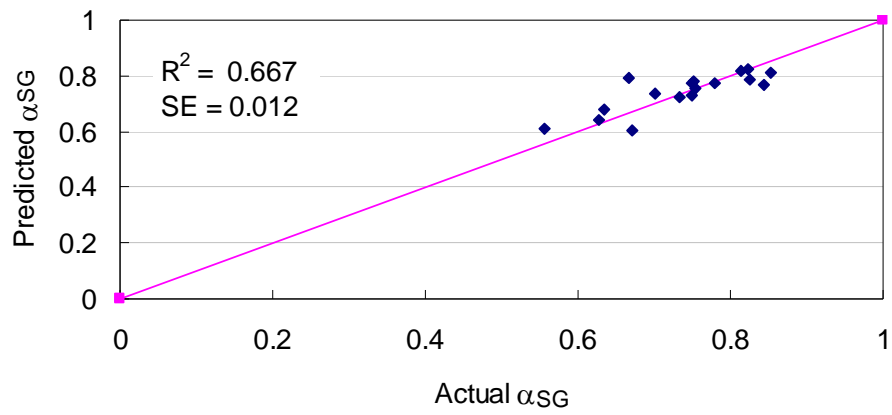


(a) α_{base}

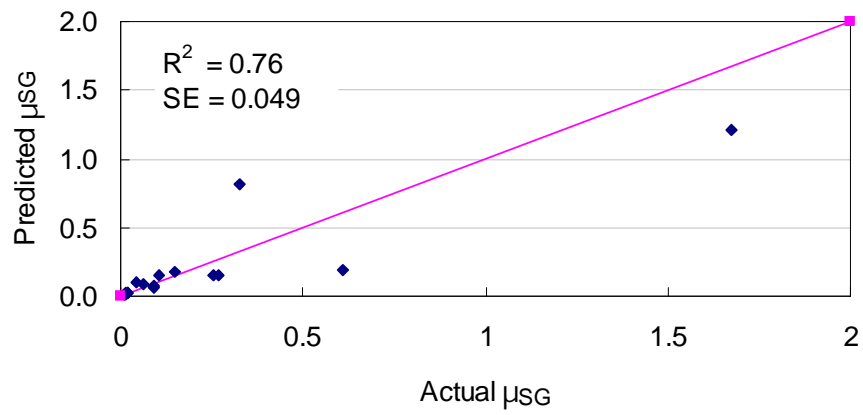


(b) μ_{base}

Figure 4 Actual versus predicted PDPs for base layer



(a) $\alpha_{subgrade}$



(b) $\mu_{subgrade}$

Figure 5 Actual versus predicted PDPs for subgrade layer

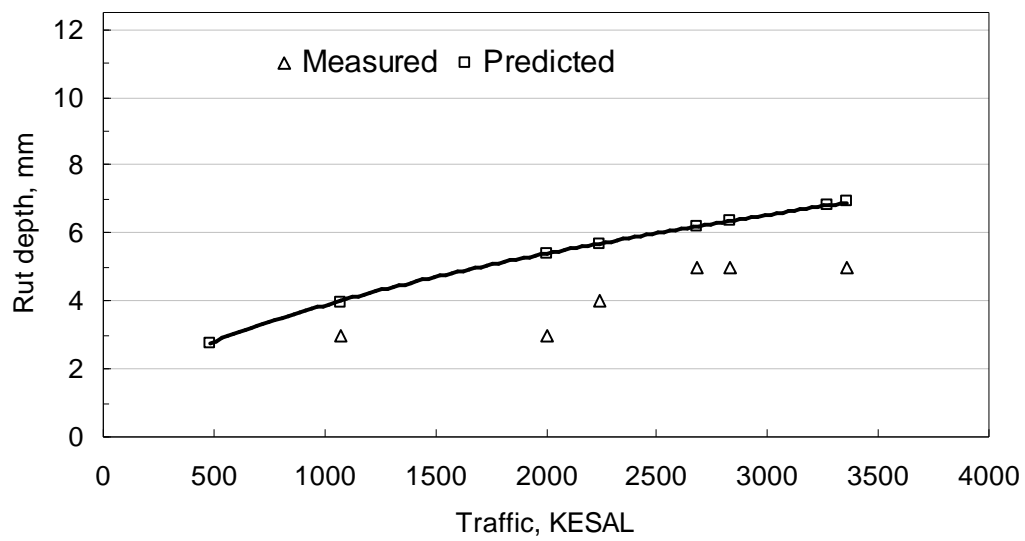


Figure 6 Field versus predicted total surface rut depth for section SPS-1 50113